Fitting Calculation of Three Dimensional Initial Geostress Field

Jing Wang

Geotechnical and Structural Engineering Research Center, Shandong University, Jinan 250061, China

1178842823@qq.com

Abstract

According to the topography, geology, in-situ stress measurement data and measured data, the three dimensional nonlinear finite element analysis model of geo-stress inversion is established. The in-situ stress field in the plant area is inversed, and the origin and distribution of the initial stress field are analyzed. Based on the results of initial geo-stress field, the initial geo-stress was studied.

Keywords

In-Situ Stress; Topography; Geology; Initial Geo-Stress.

1. Introduction

Stress is the initial stress state of rock mass. It is not only the main control factors of rock mechanical behavior, but also the source of the deformation and failure of rock mass. The formation of ground stress is complex and diverse, which is generally considered to be the result of the development of the gravity and tectonic movement of the earth plate. At the same time, it is also affected by the environment, such as lithology, topography, fault and fissure. It is closely related to the self-weight of the rock mass and geological tectonic movement, and is a function of space and time. Initial geo-stress is not only one of the most important factors affecting the stability of hydraulic structures, high slopes, underground structures and rock foundations, but also the prerequisite and basis for simulating the stress release process of excavation. Therefore, it has a great significance to simulate the initial stress field of engineering investigation field by field test and analysis.

At present, there are two kinds of methods for the inversion of initial geo-stress field: one is the displacement back analysis method, which is based on the measured displacement caused by the excavation of the site. The other is the stress regression analysis method, which is based on the understanding of the regularity of the regional crustal stress field. The method is more efficient and reliable when the initial geo-stress data are measured. In this paper, second methods are used to analyze the 3D initial geo-stress field.

2. Multiple linear regression principle of three dimensional stress field

According to the principle of multiple regression, the regression value $\hat{\sigma}_k$ of ground stress is taken as the dependent variable. The self-weight stress field and tectonic stress field calculated by the finite element method are corresponding to the calculated stress value of the measured point σ_k^i as an independent variable. The form of regression equation

$$\hat{\sigma}_k = \sum_{i=1}^{n} L_i \sigma_k^i \tag{1}$$

Where, k is the serial number of the observation point. $\hat{\sigma}_k$ regression value for the first k observation point. L_i is a multiple regression coefficient corresponding to the independent variable. $\hat{\sigma}_k$ and σ_k^i are single matrix for the measured and calculated values of the corresponding stress components. n is the number of working conditions.

If there are m observation points, the residual sum of squares of the least squares method is

$$S_r = \sum_{k=1}^{m}\sum_{j=1}^{6}(\sigma_{jk}^{*} - \sum_{i=1}^{n} L_i \sigma_{jk}^{i})^2 \tag{2}$$

Where, σ_{jk}^{*} is the observed value of j stress component of k observation point, and σ_{jk}^{i} is the finite element value of j stress component of k observation point under i condition.

According to the principle of least squares, the equation of S_r is the minimum

$$\begin{vmatrix} \sum_{k=1}^{m}\sum_{j=1}^{6}(\sigma_{jk}^{1})^2 & \sum_{k=1}^{m}\sum_{j=1}^{6}\sigma_{jk}^{1}\sigma_{jk}^{2} & \sum_{k=1}^{m}\sum_{j=1}^{6}\sigma_{jk}^{1}\sigma_{jk}^{n} \\ & \sum_{k=1}^{m}\sum_{j=1}^{6}(\sigma_{jk}^{2})^2 & \sum_{k=1}^{m}\sum_{j=1}^{6}\sigma_{jk}^{2}\sigma_{jk}^{n} \\ & \vdots & \\ & & \sum_{k=1}^{m}\sum_{j=1}^{6}(\sigma_{jk}^{n})^2 \end{vmatrix} \begin{vmatrix} L_1 \\ L_2 \\ \vdots \\ L_n \end{vmatrix} = \begin{vmatrix} \sum_{k=1}^{m}\sum_{j=1}^{6}\sigma_{jk}^{*}\sigma_{jk}^{1} \\ \sum_{k=1}^{m}\sum_{j=1}^{6}\sigma_{jk}^{*}\sigma_{jk}^{2} \\ \vdots \\ \sum_{k=1}^{m}\sum_{j=1}^{6}\sigma_{jk}^{*}\sigma_{jk}^{n} \end{vmatrix} \tag{3}$$

To solve this equation, n undetermined coefficients $L = (L_1, L_2, ..., L_n)^T$. The calculation of initial return at any point in the domain of stress superposition from the point of the condition of finite element calculation and

$$\sigma_{jp} = \sum_{i=1}^{n} L_i \sigma_{jp}^{i} \tag{4}$$

Where, j=1, 2,... , 6 corresponds to six initial stress components.

Finally, we can measure the effect of the regression calculation by the complex correlation coefficient r, and eliminate the non-significant factors by partial correlation coefficient Vi, in order to prevent the degradation of other factors.

3. Stress characteristics

In order to study the characteristics of ground stress site, were carried out 3 groups of rock stress test in the main powerhouse and main transformer house. ZKz-22, ZKz-24 and ZKz-48 test-hole lithology is mainly marble, columnar rock, joint development, by means of the testing method of hydraulic fracturing method.

Table 1. The results of spatial stress test of rock mass

Calculation results of three dimensional principal stress			
principal stress(σ_n)	Stress value(MPa)	Position	Dip angle
Maximum principal stress σ_1	12.36	204.83	18.15
Intermediate principal stress σ_2	9.78	0.44	70.07
Minimum principal stress σ3	8.98	112.20	7.95

4. Three-dimensional inversion analysis of ground stress field

The in-situ stress field regression of the plant area is calculated by using the international large-scale three-dimensional finite difference software FLAC3D and the regression analysis program. Finally, based on the stress superposition principle, the stress field in the whole study area is synthesized.

4.1 Three dimensional calculation model

In the inversion of the earth stress, the coordinate origin of the 3D initial stress field calculation model is in the position of the geodetic coordinate (X -O-Y): X0 = 516851m, Y0 =3280230m, Z0=1154m. The coordinates of the three coordinates are: Y axis and geodetic coordinates of the vertical direction (vertical upward) coincide with the axis direction of the plant is parallel to the Z axis, X vertical axis direction of the plant. The three-dimensional model is shown in Figure 3-1, the model is divided into 115037 units, the 20640 nodes. Rock mechanics parameters of surrounding rock are shown in table 2

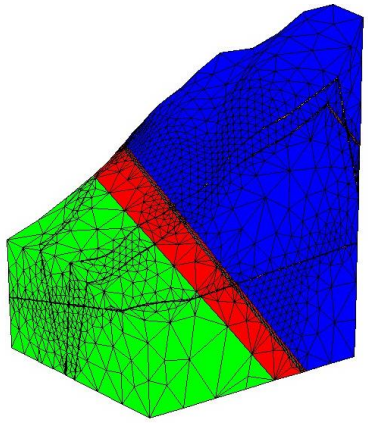

Fig. 1 3D stress calculation model

Table 2. Mechanical parameters of surrounding rock mass

Surrounding rock classification	Natural density	Tensile strength of rock	Poisson ratio	Deformation modulus	The shear strength of rock mass	
					f	c
	g/cm3	MPa		GPa		MPa
Dwg^{4-4}	2.95	6.0	0.29	5.0	38	0.7
Dwg^{4-3}	2.81	5.0	0.28	7.0	40.0	0.8
Dwg^{4-2}	2.61	10.0	0.25	12.0	50.0	1.5
Fault	2.40	1.5	0.36	0.8	20.0	0.05
Alteration zone	2.40	1.5	0.36	0.8	20.0	0.05

4.2 Multiple regression analysis

(1) Calculation conditions

Firstly, the principal stress and the principal stress direction of the in-situ stress data are converted to the 6 stress components in the calculated coordinates. Then determine the stress field formed by fitting the load structure model as follows: self-gravity, the tectonic force, the X direction in the Z direction, the extrusion tectonic stress in XZ direction of tectonic stress in ZX, shear to shear structure.

(2) coefficient regression

Table 3. Comparison of calculated and measured values of ground stress (MPa)

Measuring point number		The first principal stress	Second principal stress	Third principal stress
ZKz-22	measured value	12.36	9.78	8.98
	calculated value	14.31	9.95	6.05
ZKz-24	measured value	12.36	9.78	8.98
	calculated value	14.74	10.09	3.68
ZKz-48	measured value	12.36	9.78	8.98
	calculated value	13.48	7.70	4.08

4.3 Analysis of the characteristics of regression in-situ stress field

By the influence of gravity field, horizontal tectonic movement, fault and so on, it can be seen that the measured value and the regression value are similar from the measured values of the principal stress and the regression value. Generally speaking, the calculated value of the first principal stress is larger than the measured value, and the calculated value of the third principal stress is smaller than the measured value, which is not conducive to the stability of the surrounding rock. Figure 2 -9 gives the main stress distribution contour map of the 1# section, 2# unit, 3# unit and 4# unit in the plant area.

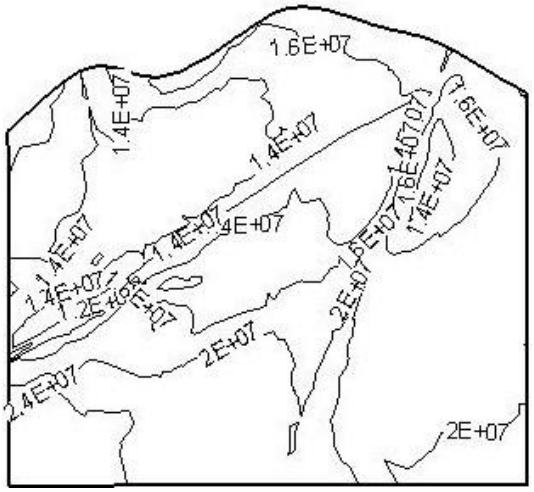

Figure 2. Contour map of maximum principal stress of 1# unit section

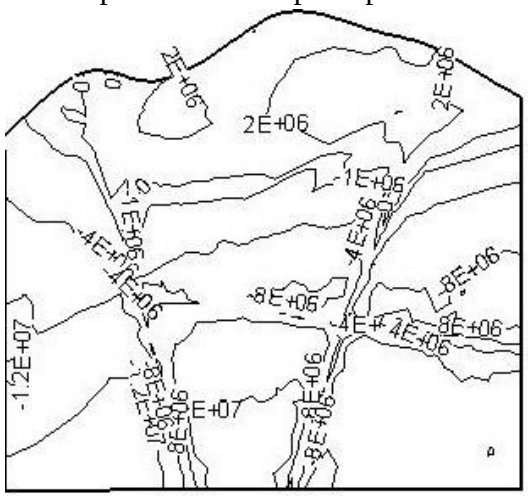

Figure 3. Contour map of minimum principal stress of 1# unit profile

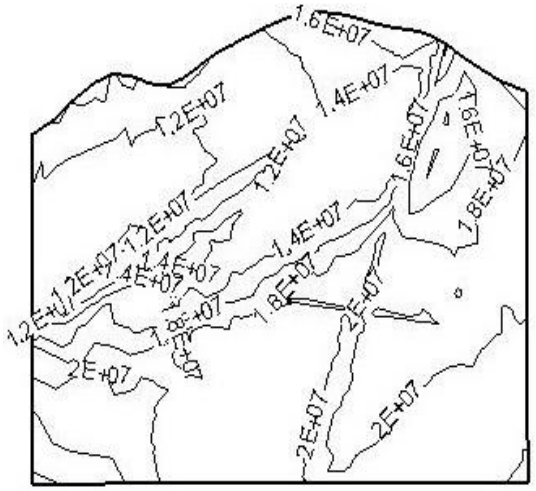

Figure 4. Contour map of maximum principal stress of 2# unit section

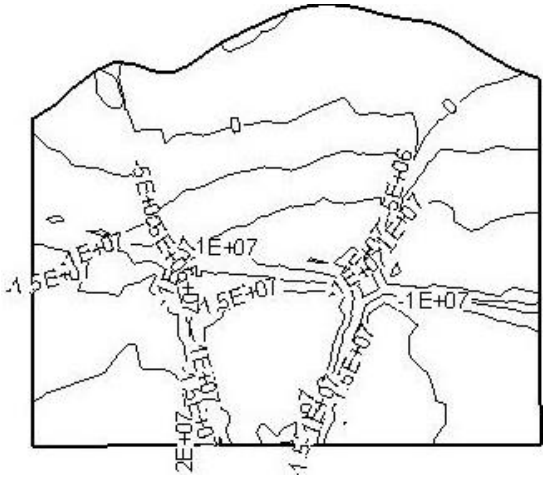

Figure 5. Contour map of minimum principal stress of 2# unit profile

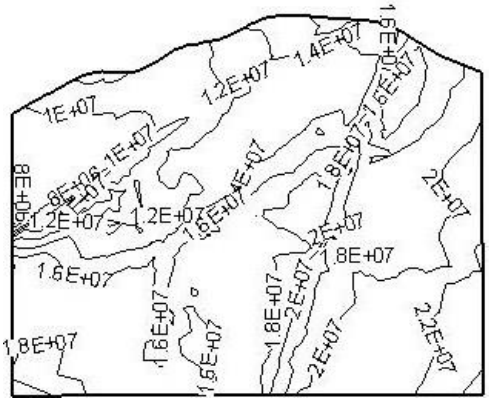

Figure 6. The contour map of maximum principal stress of 3# unit surface

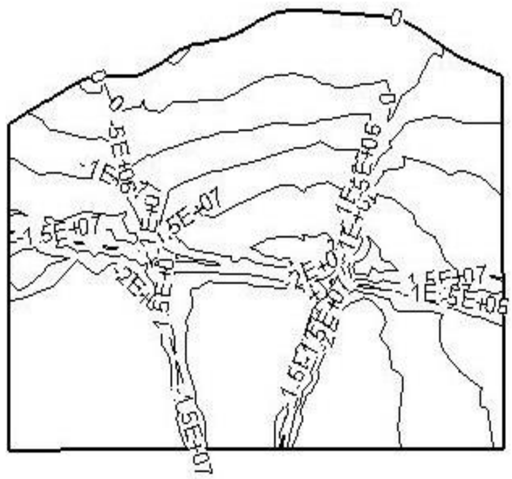

Figure 7. Contour map of minimum principal stress of 3# unit profile

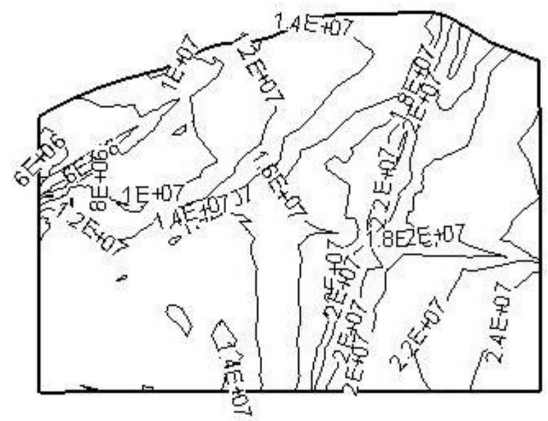

Figure 8.The maximum principal stress contour map of 4# unit

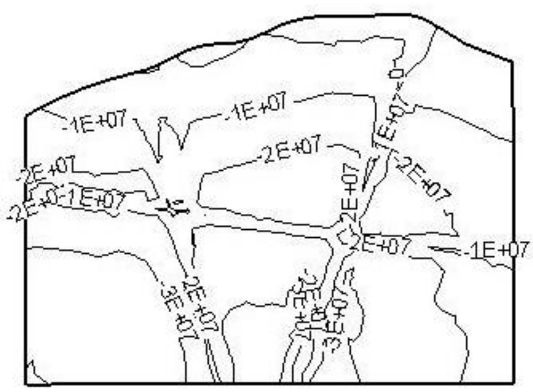

Figure 9. The minimum principal stress contour map of 4# unit

The maximum principal stress is close to the horizontal direction, and the minimum principal stress is close to the vertical direction, Figure 2-9 gives the plant area of the four units of the main stress distribution potential line map.

(1) We can see from the distribution of the principal stress contour of each surface: the value of the principal stress is gradually increased from the top to the bottom, and the isocline is affected greatly by the change of the terrain. It is shown that the inversion of the stress field is a reflection of the influence of topography and geomorphology.

(2) In the fault zone, which is affected by the compression and shear of the fault (which only reflects the tendency of extrusion) in the numerical calculation, the initial stress in the area is characterized by the

change of stress. Due to the existence of the fault and the deformation modulus of the fault, the stress gradient of the rock mass is larger and the stress value is smaller. On the two sides of the fault, the stress isocline is wrong.

(3) In stability calculation, calculate the application of lateral pressure coefficient. Select the plant area of center point calculation of lateral pressure coefficient, the maximum principal stress at this point is 9.27Mpa, the intermediate principal stress is 7.47Mpa, the minimum principal stress is 6.16Mpa. The lateral pressure coefficient is perpendicular to the axis of the building about 1.5. In parallel to the axial direction of the plant is about 1.2.

5. Conclusion

The plant area of geo-stress regression using large-scale three-dimensional finite difference international general calculation software FLAC3D and regression analysis were calculated, based on obtained throughout the study of regional stress field stress superposition principle. The following conclusions are obtained

(1) Using the stepwise regression method, the basic factors that influence the crustal stress field and the measured data are selected. The regression results are closer to the actual stress field, and the uniqueness of the solution of the stress field is guaranteed as far as possible. Through the calculation of the stress value and actual value comparison and comprehensive analysis of the law of the lateral pressure ratio. The results show that the initial stress field can reflect the influence of topography, geomorphology and geological structure. The result has good reliability. It can be used as reference for design, construction and stability evaluation.

(2) Intuitively, the lateral pressure coefficient is perpendicular to the axis of the building about 1.5, while in parallel to the axial direction of the plant is about 1.2

References

[1] Oda M.Permeability tensor for discontinuous rock masses[J].Geotechnique.1985,35(4):483-495.
[2] BEAR J.Dynamics of fluids in porous media[M].New York:Elsevier, l972.
[3] Oda M.An equivalent continuum model for coupled stress and fluid flow analysis in jointed rock masses[J].Water Resources Research.1986,22(13):1845-1856.
[4] Long J C S.Porous media equivalents for networks of discontinuous fractures[J].Water Resources Research,1982,l8(3): 645-658.
[5] Peng S,Johnson A M. Crack growth and faulting in cylindrical specimens of Chelmsford granite. International Journal of Rock Mechanics and Mining Sciences & Geomechanics Abstracts , 1972, 9(1): 37-86
[6] Y. Liu, Z. Chen, S. Li, J. Zhang, J. Gao Energy education scinence and technology PART A Volume 29 (1) April 2012. Experimental study on mechanical characteristic of weak interlayer in red-bed soft rock slope 467-474
[7] Griffith A.A. The theory of rupture [C]. Proc.1st Int. Congr. Applied Mech., Delft,1924:55-63.
[8] J. Wang, W. Tang, Y. Li, Y. Shen.Energy education scinence and technology PART A Volume 30 (1) October 2012
[9] Nolen-Hoeksema R.C. and Gordon R.B.Optical detection of crack Patterns in the opening-mode fracture of marble [J].Int. J. Rock mech. Mn. Sci. Geomech. Abdtr. 1987,24(4): 135-144.
[10] Sommer E. Formation of Fracture ‘lances’ in Glass[J]. Engineering Fracture Mechanics,1969,1: 539-546.